Guided waves for structural health monitoring

O. Mesnil, B. Chapuis, Tom Druet

HAL Id: cea-01843008
https://cea.hal.science/cea-01843008

Submitted on 2 Jun 2021

Guided waves for Structural Health Monitoring

Olivier Mesnil, Bastien Chapuis and Tom Druet
CEA Tech, Institut LIST
Gif-sur-Yvette, France
+33 1 69 08 58 28
Olivier.mesnil@cea.fr

Abstract

Structural Health Monitoring (SHM) consists in permanently installing sensors onto or into a structure in order to monitor its health without disturbing its regular operating cycle. Guided wave (GW) based SHM relies on the propagation of GWs in plate-like or extruded structures. Because of their high sensitivity to geometrical singularities, GWs are suitable to detect structural flaws. Moreover, because GWs can be generated and measured with lightweight low-energy sensors such as piezoelectric sensors, GWs are often the ideal interrogation mean to detect and locate flaws in a SHM context.

Despite the large literature on the use of GW for SHM, no GW-based SHM systems have yet reached a sufficient maturity level to be deployed in large scale industrial applications. The CEA-LIST conducts a substantial number of studies aiming at transferring these technologies from the laboratory towards the industry. This work includes the development of novel simulation tools, the improvement of existing imaging techniques along with their implementation on complex cases, the use of optical fibers to replace or complement piezoelectric sensors and limit the mass of the SHM system and the development of new GW-based techniques. This communication will describe these developments along with the perspectives of this work.

1. Introduction

Structural Health Monitoring (SHM) is the discipline of permanently installing sensors onto or into a structure in order to continuously or periodically monitor its health in a non-destructive fashion. As an SHM system is made to remain with the structure during its life cycle, it is crucial that an SHM system does not disturb the operating cycle of the structure it is meant to inspect. Driven mainly by aerospace actors, multiple industries may achieve significant maintenance cost reduction with SHM. Beyond the fact that SHM must fulfil similar requirements as traditional non-destructive evaluation techniques (such as the performances of detection), SHM faces others challenges such as the integration of the SHM system (size, mass and energy efficiency), the robustness of the detection in various environmental conditions, the life cycle of the integrated system itself, along with its economic viability. As of summer 2017, a single SHM system is certified to fly on an aircraft for the reason that it is extremely difficult to meet all the aforementioned requirements.

Multiple physical quantities may be monitored to assess the health of a structure and among them, Guided Waves (GWs) are particularly promising. GWs are elastic waves propagating in waveguides, for example unidirectional extruded features (ex: rails, pipes)

or plate-like structures, which are the leading structures in most industries. Among the advantages of GW for SHM, it must be noticed that GW are extremely sensitive to defects and propagate over long distances with a small input energy requirement making them suitable for an SHM configuration (limited number of sensors). The main downsides of GW are the facts that they are also sensitive to boundary conditions, are multi-modal and dispersive, making them complicated to analyze, and are sensitive to environmental conditions.

A broad literature is available on GW-based SHM (GW-SHM) and a large number of techniques have been proposed to detect a wide panel of defects in various structures. For example GW Imaging (GWI) consists of creating an image of the inspected structure through the measure of propagated GWs. Most often, but not necessarily, GWI relies on an array of piezoelectric (PZT) transducers, each acting sequentially as emitter and receiver of GW in order to measure the propagated wave packets between every pair of sensors. In this configuration, it is assumed that the presence of a defect will somehow modify the propagation of waves, for example with the existence of a reflected wave packet. Other GW techniques include acoustic emission, beamforming, pulse echo and tomography. Current limitations of GW-SHM techniques are based on the fact that GWs are very sensitive to a large number of parameters and it is therefore difficult to separate the influence of defects in the measured signals from the influence of other parameters such as the variation of temperature or varying boundary conditions.

The underlying motivation for the various SHM projects conducted at the CEA-LIST is to better understand GW propagation phenomena to propose systematic and robust signal measurement and analysis techniques to evaluate defects in a reliable, robust and repeatable fashion. First, numerical tools combining the recent advances in finite element analysis and specially dedicated towards GW simulations are developed. The objective of these tools is to be able to run extensive simulation campaigns in order to better understand the interconnectivity of the various influent parameters, leading to conclusions on how to work with them in the field. Secondly, various GWI techniques, each using different physical metrics to detect and locate defects, are implemented to be compared. The goal being to propose criteria on how to choose one technique or another in a given situation. Next, a baseline free GW tomography technique is developed in order to finely monitor regions with high presence of defects with no knowledge of the initial condition. Finally, the feasibility of the use of optical fibres to measure and reconstruct GW from the ambient noise is demonstrated and could lead to various applications with no need for an external energy input.

2. Numerical tools for Guided Wave based Structural Health Monitoring

The need for numerical tools in GW-SHM arises from the high sensitivity of GWs to a large set of parameters, such as the temperature, the defect shape/location or even the quality of the bounding between each sensor and the inspected sample. Indeed, due to the potential variability of GW signals between two seemingly identical configurations, a very large number of experiments would be necessary to qualify the performances of an SHM system in a given situation (e.g. through the determination of Probability of Detection (POD) curves). Numerical tools provide the means to study a wide number of

configurations at a limited cost. However, GW are recognized to be computationally intensive to simulate numerically. Indeed, in classical Finite Element (FE), the simulation of GW generally requires small computational time steps along with a small spatial discretization, leading to cumbersome simulations. The main objective of the tools presented in this section is to simulate GW in a computationally efficient manner. The first tool, a hybrid modal finite element tool, is already released and available in the commercial software CIVA and is especially efficient, but not limited to, the simulation of GW in unidirectional extruded features. The second tool, a transient spectral finite element tool, is currently in development and is dedicated to the simulation of GW in plate-like anisotropic structures with various features.

2.1. Hybrid modal finite element tool for GW

The hybrid modal finite element tool, also called the Guided Wave Module in the commercial release of CIVA, is a GW simulation tool with three main functionalities. First, this tool is able to compute the dispersion relations of any waveguide based on a Semi-Analytical Finite Element (SAFE) formulation [1]. Secondly, and based on this formulation, the displacement induced by a GW in the cross section of any waveguide can also be computed. Finally, this tool is able to compute the GW response to any perturbation, which could represent a flaw, a change of geometry or a junction of multiple geometries for example. This last step is achieved by a FE solver in the frequency domain. The key advantages of this tool are to reduce the size of the FE region in order to minimize the computational cost and to ensure communication between the FE region and the modal region through transparent boundary conditions. An example of a use case is represented in Figure 1a in which a rail is considered. In a region of this rail, two cracked holes and three eroded regions are created and represented by the red features in Figure 1a. The signal transmitted between the emitter (E) and the receiver (R) can then be computed. Note that pulse-echo configurations are also available. For illustration purposes, the excitation and the measurement signals are represented Figure 2. This tool allow the computation of this configuration for various parameters such as sensor positioning, defect size/shape, local change of material, change of cross section or the computation of GW passing through an intersection of multiple waveguides. For more information about this tool, the reader is invited to refer to [2] and [3].

(a)   (b)
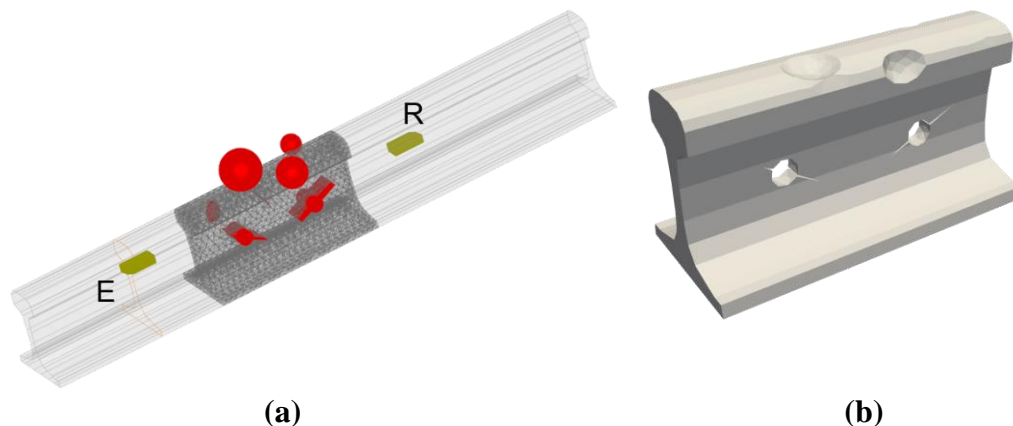
Figure 1: Geometry of interest in the hybrid modal finite element tool. (a): a rail with two sensors (E and R) and multiple features represented in red. The FE box is limited to the region containing the features and (b): Resulting geometry in the FE box.
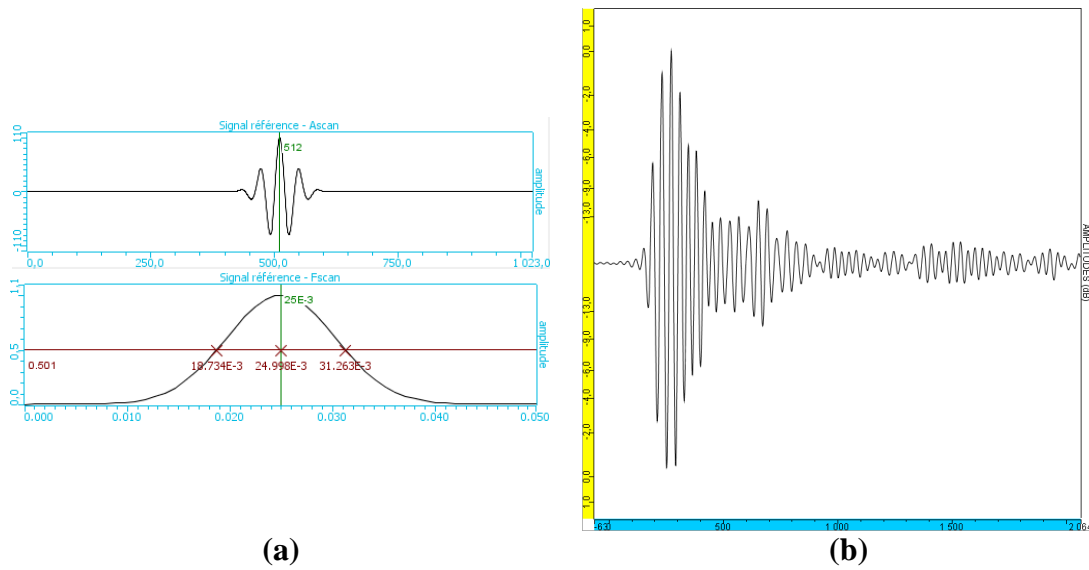
(a)   **(b)**

Figure 2: (a): Excitation signal sent by E in Figure 1: 25 kHz tone burst and (b): Received signal at R.

2.2. Transient spectral finite element tool for GW

A tool based on transient spectral finite elements is currently under development at the CEA-LIST. This tool rely on spectral finite elements [4] to simulate GW propagation using high order spatial elements, thus, reducing the number of degrees of freedom compared to classical FE. The formulation adopted in this tool is especially oriented towards the accurate and efficient simulation of GWs in an SHM context. For illustration purposes, the simulation of composite panel excited by a piezoelectric transducer with a tone-burst at 100 kHz is represented in Figure 3. The formulation allows the simulation of any anisotropic materials with various features such as the presence of stiffeners or a curvature, as well as the presence of various flaws such as holes, thickness reduction, cracks or delaminations. For more information about this tool, the reader is invited to refer to [5].

(a)   (b)

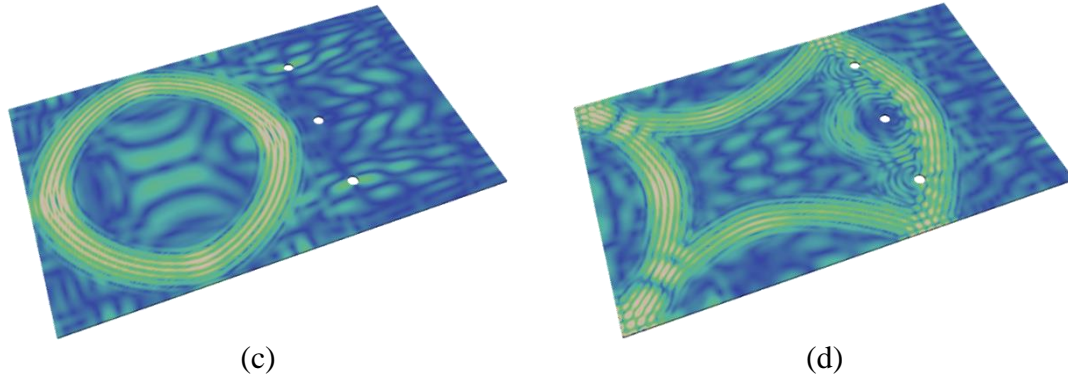(c)   (d)
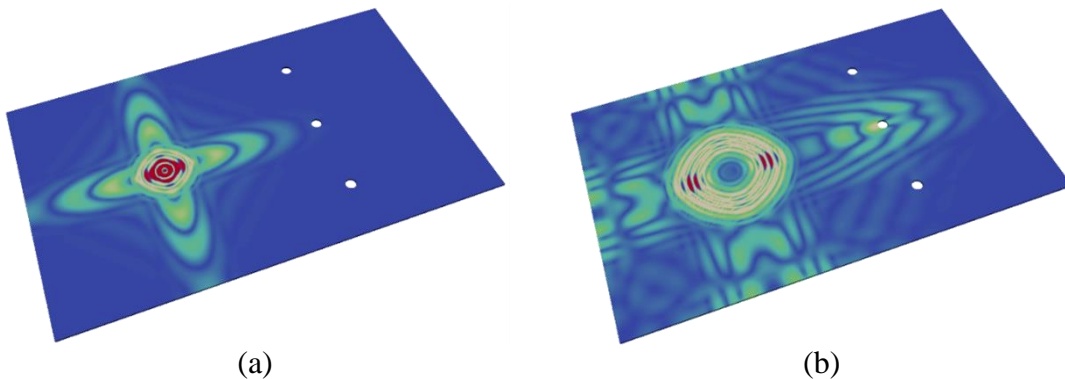
Figure 3: GW propagation simulated with the transient spectral finite element tool in an anisotropic plate with three holes at various time steps (a): 26 μs, (b): 44 μs, (c): 87 μs, and (d): 140 μs [5]

3. Guided Wave Imaging

Guided Wave Imaging (GWI) is based on the measurement of an array of transducers (often piezoelectric transducers) sequentially emitting and receiving GWs. These measurements are then interpreted using some knowledge of the physics of the propagation of the GW in the medium in order to create an image of the inspected specimen. These images represent a metric based on the health of the structure and singularities in the images are expected at the location of the unexpected features such as flaws. Most GWI techniques rely on the knowledge of the GW signals in a pristine state, known as baseline, in order to isolate the acoustic response of the potential flaws. Indeed, as GWs are multi modal and dispersive, their analysis is often delicate and it is rarely possible to directly identify the wave packets reflected by a mild defect among the GW measurement. The difference between a baseline signal and a signal measured in an unknown state is called residual signal. Various algorithms using different metrics to detect defects using knowledge about the physics of the wave propagation to interpret the signals are available in the literature. As a rule of thumb, the more physics is used by an algorithm, the better the imaging result but the more difficult the algorithm is to apply to complex cases. The algorithms used in this document are summarized in Table 1.

Table 1: Guided Wave Imaging algorithms

Algorithm	Inputs from the physics	Process	Comment
RAPID (Reconstruction Algorithm for Probabilistic Inspection of Damage) [6]	None.	Correlation between baseline signal and signal in current state for each pair of sensor.	Rough probability of presence of a defect in a wide area.
DAS (Delay-and-Sum) [7]	Group speed of the dominant mode at the dominant frequency.	Residual signal is delayed by the theoretical time of flight to triangulate	Simple yet efficient algorithm to detect defects and obtain a rough estimation of their locations.

		the source of the reflected waves.	
MV (Minimum Variance) [8]	Same as DAS and scatter directivity (optional).	After applying DAS, minimization is applied to the image to reduce noise and false alarms.	Improvement of DAS based on image analysis. Further improvement possible if the scattering pattern of the searched defect is known.
Excitelet [9]	Dispersion relations in the relevant frequency range.	Residual signal is correlated to the theoretical signal for each potential defect pixel. High correlation means presence of a defect.	Precise and accurate, but computationally intensive defect detection and localization.

For comparison purposes, the images obtained by the four algorithms are presented in Figure 4 for the following configuration: 8 piezoelectric sensors are glued to a 400x400x3 mm³ aluminium plate and are sequentially excited by a 2-cycle 40 kHz sine burst while the other sensors measure the propagated GWs. This measurement is first done in a pristine state then a 10 mm diameter hole is drilled near the centre of the plate and the same measurement process is repeated. The baseline signal and the signal measured in the presence of the defect are then fed to the algorithms leading to the pictures of Figure 4. All algorithms except RAPID (Figure 4a) detect and locate satisfyingly the defect, while DAS is slightly less precise than the last two. The existence of a defect is roughly detected by RAPID as well.

(a)   (b)

<div align="center">(c)</div>
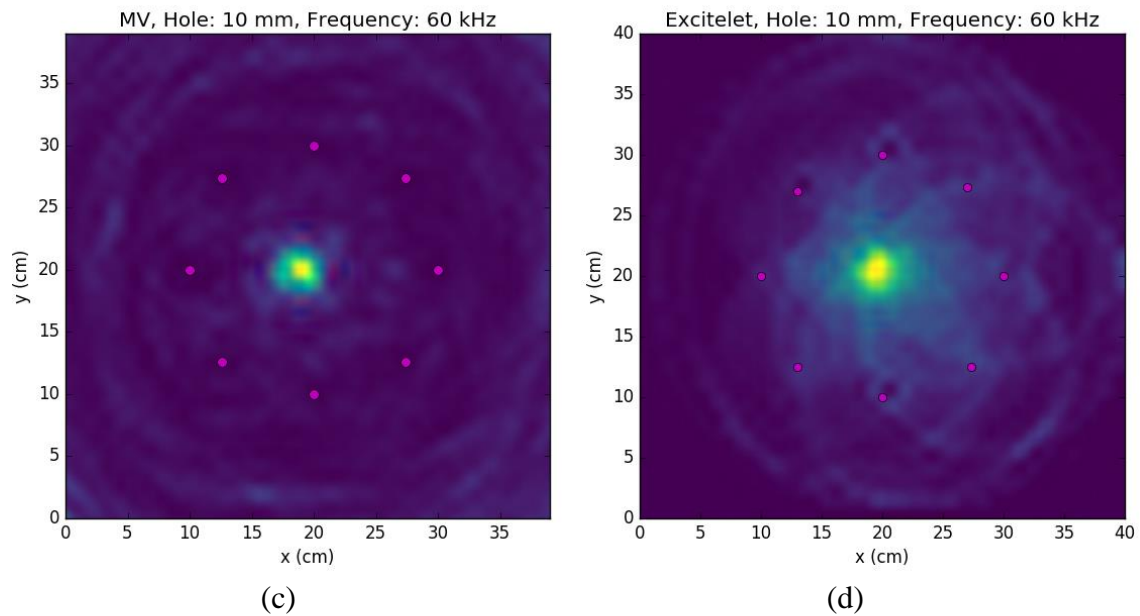
<div align="center">(d)</div>
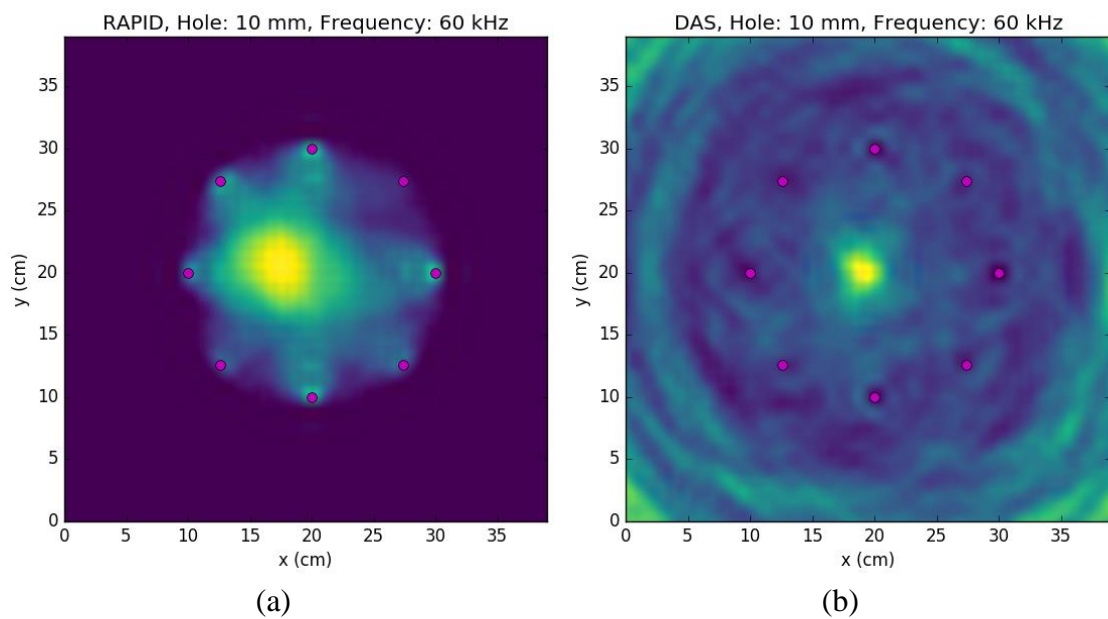
Figure 4 : Comparison of the GWI algorithms (a) : RAPID, (b): DAS, (c): MV (assumption: omnidirectional scatter) and (d) : Excitelet applied to a 400x400x3 mm aluminum plate instrumented by 8 piezoelectric transducers (pink dots) with a 10 mm diameter hole (actual hole location (x,y) = (19,20))

Despites the successful imaging in the previous case, these algorithms cannot be applied blindly to any dataset, even using the baseline subtraction operation. Indeed, in the cases of DAS, MV and Excitelet, it is assumed that the reflected wave packets travel directly from the defect to the transducers. If the inspected structure has geometrical singularities reflecting wave packets in its design such as stiffeners or rivets holes, these features will induce additional reflections leading to false alarms in the cartography. Moreover, using any of these three algorithms require to know the physics of the GW propagation, which may be hard to obtain in the case of unknown material properties. RAPID, because it does not use any input from the physics besides the measurements themselves, can be applied in any situation regardless of the geometrical features or the anisotropy of the inspected structure.

As an example, an algorithm based on RAPID is applied to an aircraft wing represented in Figure 5a. The sample is anisotropic and the material properties and the dispersion relations are unknown. Furthermore, nine stiffeners (7 horizontal and 2 vertical) are present on this sample. The algorithms DAS, MV and Excitelet cannot be easily applied to this situation, even when using a perfect baseline signal due to the multiple reflections of the wave packets. The specimen is instrumented by 16 piezoelectric transducers and a defect is simulated by placing 2 magnets on either side of the specimen in the top right corner. The resulting image is represented in Figure 5b, in which the defect (true location represented by a red dot) is successfully detected and roughly located.
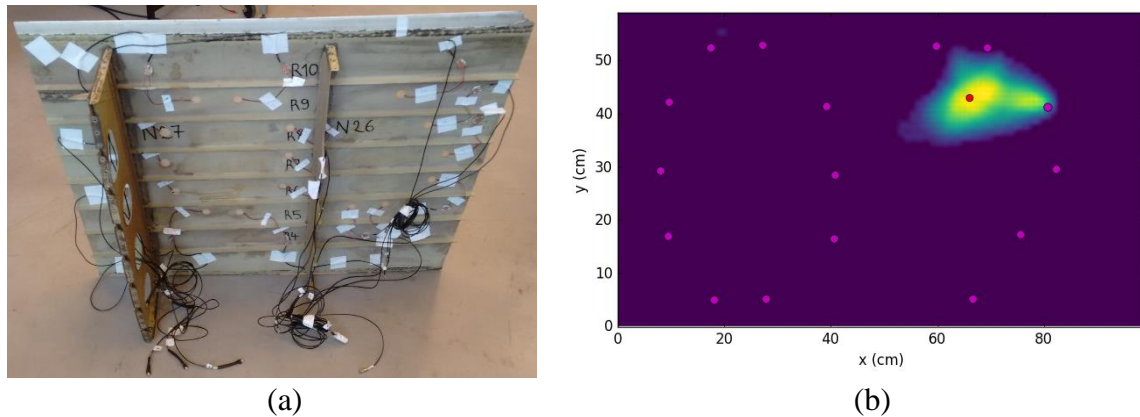
Figure 5 : Application of an algorithm based on RAPID to inspect a defect (added magnetic mass) on an piece of an anisotropic aircraft wing with multiple stiffeners (a): specimen and (b) result, the position of the 16 piezoelectric sensors is specified by the pink circles while the defect is located by the red dot

4. Baseline free GW tomography

The need for a baseline signal is widely recognized to be the main limitation of GWI in realistic use cases. Indeed, any variation of an experimental parameter such as temperature or sensor positioning will induce a significant change in the signals leading to potential false alarms. Therefore, the baseline and the signal in the potentially damaged state must be taken on the same specimen in nearly identical environmental conditions and the performances of the sensors must remain the same between the two states. In practice, various strategies have been proposed to loosen this requirement. Mainly focusing on compensating temperature effects, these processes are limited in term of range of application and are not able to take into account all the potential signal variations, such as sensor aging. In parallel, baseline free techniques are being developed for simple application cases, but remain limited in the inspection of complex geometries [10]. Among those techniques, baseline free GW tomography show great promises.

GW tomography algorithms aim at reconstructing a 2D image of an inspected area based on 1D projections (i.e. GW measurements between an emitter and a receiver) obtained from a distribution of sensors. The example used in this section is a 60-cm diameter circle of 30 piezoelectric transducers integrated on a 2-mm thick aluminium plate as pictured in Figure 6a. On this plate, a thickness loss up to about 0.65mm was manufactured to represent a corroded area. Based on the measure of the time of flight between every pair of sensors, and on a straight-ray algorithm [11] [12], the tomography allows the reconstruction of the local wave propagation speed values for the entire area within the sensors circle. Based on the knowledge of the dispersion relations of the specimen (i.e. the group speed as a function of the frequency-thickness product), the residual thickness can be quantified as represented in Figure 6b. Besides the knowledge of the dispersion curves of the material, no baseline was used to obtain this result and the accuracy of this result is of the order of 0.1mm. This technique is particularly promising for the inspection of "hot-spots", or areas of a structure known to be origin of mechanical failures.
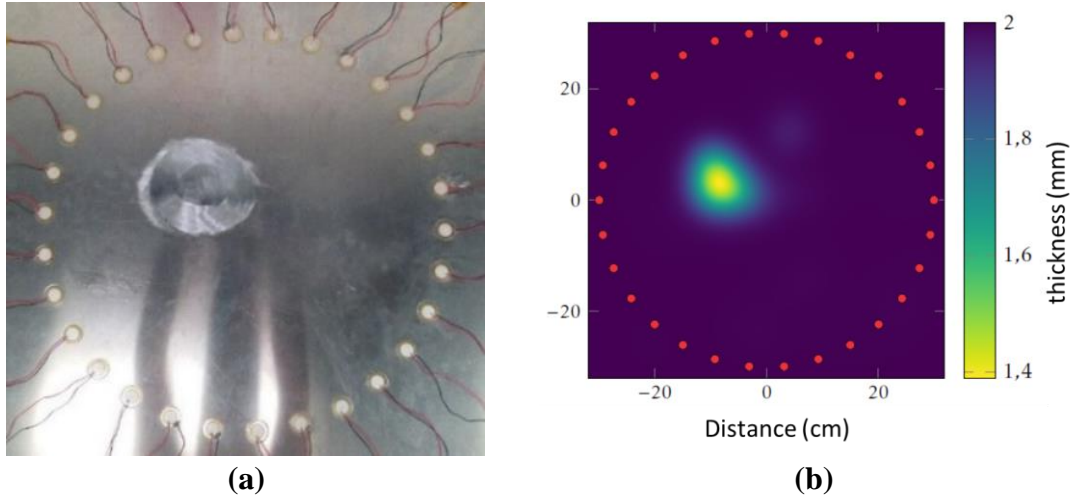
Figure 6: GW tomography (a): corroded aluminium plate instrumented by 30 sensors and (b): estimated thickness loss [12]

Passive approaches rely on the measurement of the ambient noise from various sensors and correlation-based operations to compute a GW signal for a pair of sensors, equivalent to a GW originating from an active source. The tomography methodology discussed in this section has also been implemented in a passive setup, i.e. no energy input is used to generate GWs [13]. Passive methodologies are of great interest, especially thanks to the emergence of optical fibers as GW sensors.

5. Passive GW measurement by optical fiber

Piezoelectric transducers are commonly used within the GW community because of their low cost and versatility. One of the main limitation of these sensors is the need for individual cables for each sensors, leading to complex wiring issues and significant added mass for applications requiring hundreds of sensors. Optical fibers equipped Fiber Bragg Grating (FBG) is a very promising unidirectional sensor to measure GW because of scalability and near-zero added mass [14] [15]. Unlike piezoelectric transducers however, FBG can only be used as a GW receiver making them particularly suitable for passive GW approaches.

In Figure 7 the wave packets received by a FBG and a piezoelectric transducer is represented for various location of the transducer. These wave packets have been reconstructed from the ambient noise present in a 2-mm thick aluminum plate. The ambient noise was created in the structure by spraying compressed air on the structure at random locations. Note that both FBG and piezoelectric transducer only act as receiver and the piezoelectric transducer is only used because more convenient than another FBG to move at multiple locations to study various distances but was not used actively. In this result, the propagation effect is clearly visible, as the time of flight increases linearly with the distance of propagation and the time of flight matches the theoretical dispersion curves.
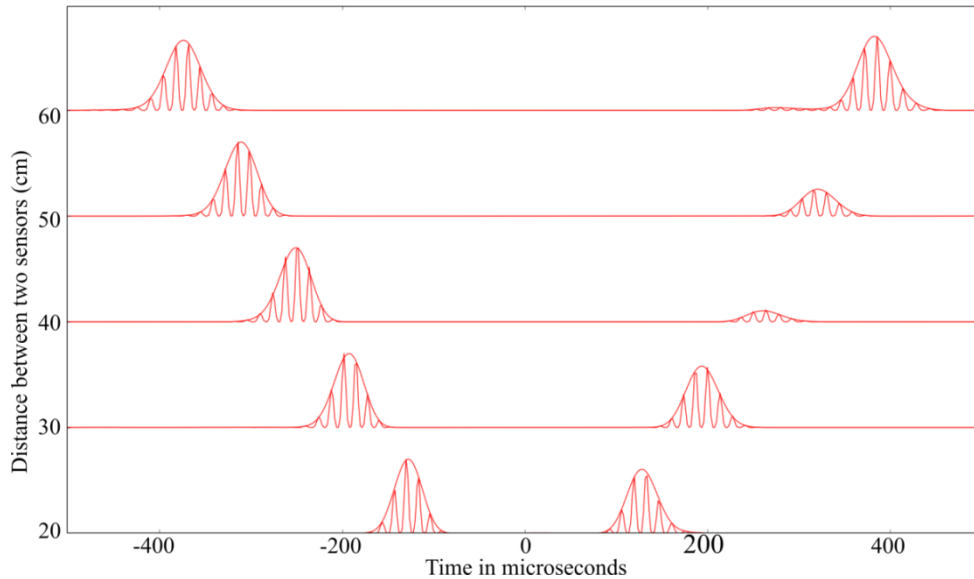
Figure 7: Reconstruction of passive signals between a piezoelectric transducer and a Fibre Bragg Grating. Both transducers act only as receivers [16].

6. Conclusion

The activities of the CEA-LIST in GW-based SHM have been presented in this communication. First, numerical tools to efficiently simulate GW propagation in SHM configurations are developed and optimized for large-scale use. These tools are progressively released within CIVA software versions and will be coupled in the near future with the statistical module of CIVA in order to allow model-assisted determination of POD curves of GW-based SHM systems. Various GW Imaging algorithms described in the literature have been implemented and compared in order to establish criteria on their respective fields of application. New baseline free GW-based tomography have been developed and finally the feasibility of passive GW measurement through optical fibres has been demonstrated. The combination of the last two development would lead to the development of a new passive baseline free SHM system based on optical fibres.

Bibliographie

[1] I. Bartoli, A. Marzani, F. L. di Scalea and E. Viola, "Modeling wave propagation in damped waveguides of arbitrary cross-section," *Journal of Sound and Vibration,* vol. 295, no. 3, pp. 685-707, 2006.

[2] V. Baronian, A. Lhemery and K. Jezzine, "Hybrid SAFE/FE simulation of inspections of elastic waveguides containing several local discontinuities or defects," in *AIP Conference Proceedings*, 2011.

[3] V. Baronian and K. Jezzine, "Simulation of NDT Inspection in 3D Elastic Waveguide Involving Arbitrary Defect," 2016.

[4] G. C. Cohen and L. Qing Huo, "Higher-order numerical methods for transient wave equations.," The Journal of the Acoustical Society of America, 2003.

[5] O. Mesnil, A. Imperiale, E. Demaldent, V. Baronian and B. Chapuis, "Simulation tools for guided wave based Structural Health Monitoring at CEA LIST," in *QNDE*, Provo, 2017.

[6] X. Zhao, H. Gao, G. Zhang, B. Ayhan, F. Yan, C. Kwan et J. L. Rose, «Active health monitoring of an aircraft wing with embedded piezoelectric sensor/actuator network: I. Defect detection, localization and growth monitoring,» *Smart materials and structures,* vol. 16, n° %14, p. 1208, 2007.

[7] J. E. Michaels, «Detection, localization and characterization of damage in plates with an in situ array of spatially distributed ultrasonic sensors,» *Smart Materials and Structures,* vol. 17, n° %13, p. 035035, 2008.

[8] J. S. Hall and J. E. Michaels, "Minimum variance ultrasonic imaging applied to an in situ sparse guided wave array," *IEEE transactions on ultrasonics, ferroelectrics, and frequency control,* vol. 57, no. 10, pp. 2311-2323, 2010.

[9] N. Quaegebeur, P. Masson, D. Langlois-Demers and P. Micheau, "Dispersion-based imaging for structural health monitoring using sparse and compact arrays," *Smart Materials and Structures,* vol. 20, no. 2, p. 025005, 2011.

[10] B. Park, H. Sohn et P. Liu, «Accelerated noncontact laser ultrasonic scanning for damage detection using combined binary search and compressed sensing,» *Mechanical Systems and Signal Processing,* vol. 92, pp. 315-333, 2017.

[11] A. C. Kak et M. Slaney, Principles of computerized tomographic imaging, SIAM, 2001.

[12] P. Huthwaite and F. Simonetti, "High-resolution guided wave tomography," *Wave Motion,* vol. 50, no. 5, pp. 979-993, 2013.

[13] T. Druet, B. Chapuis, J.-L. Tastet and E. Moulin, "Guided wave tomography for corrosion monitoring in planar structures," *IWSHM,* 2017.

[14] D. C. Betz, G. Thursby, B. Culshaw and W. J. Staszewski, "Acousto-ultrasonic sensing using fiber Bragg gratings," *Smart Materials and Structures,* vol. 12, no. 1, p. 122, 2003.

[15] Y. Botsev, E. Arad, M. Tur, I. Kressel, U. Ben-Simon, S. Gail and D. Osmont, "Structural health monitoring using an embedded PZT-FBG ultrasonic sensor array," in *Proc. Fourth European Workshop on Structural Health Monitoring, Cracow*, 2008.

[16] T. Druet, M. Jules, B. Chapuis, G. Laffont et E. Moulin, «Towards Passive Guided Wave Tomography of Extended Defects Using Ambient Elastic Noise Cross-correlations,» *IWSHM 2015,* 2015.